MAGNETIC COUPLING AND TOPOLOGICAL CHANGE

Sami K. Solanki

Max-Planck-Institut für Aeronomie, 37191 Katlenburg-Lindau, Germany
tel: +49 5556-979-325 / fax: +49 5556-979-190
e-mail:solanki@linmpi.mpg.de

ABSTRACT

Magnetic field lines thread the convective layers of the Sun's interior and its atmosphere. They couple these parts of the Sun in the sense that energy is transported from the Sun's interior and surface into its atmosphere, where it is deposited, leading to a heating of the gas present there. One way of energy release is through magnetic reconnection, which leads to a change of the magnetic topology. Both these topics are briefly discussed and some recent results are reviewed, including, new measurements of the magnetic vector near the base of the corona which reveal the magnetic structure of loops and have led to the first detection of a magnetic current sheet in the solar atmosphere.

Key words: Sun: magnetic field - Sun: corona - Sun: chromosphere.

1. INTRODUCTION

The magnetic field of the Sun plays the dominant role in structuring and heating the solar corona and the transition region. It is also responsible for producing the many energetic and transient features which characterize the coronal and transition region plasma, such as flares, CMEs, X-ray jets, X-ray bright points, blinkers and explosive events.

The role ascribed to the magnetic field is to transport the abundantly present energy from the solar interior into the upper solar atmosphere, releasing it there. The magnetic field lines, some of which thread all layers from the solar convection zone right out to the heliosphere, thus couple these regions with each other. This coupling goes beyond just the transport of energy. For example, magnetic field lines also transport angular momentum and force the circumsolar gas to co-rotate with the Sun up to a distance of the Alfvén radius. Within this distance the magnetic energy density dominates over the kinetic energy density of the gas, beyond it the opposite is the case. In this sense the magnetic coupling of the solar interior to the heliosphere is responsible for the relatively low rotation rate of the present-day Sun and for the efficient loss of angular momentum from the rapidly rotating young Sun (e.g. Mestel and Spruit, 1987; MacGregor and Charbonneau, 1994; Solanki et al., 1997). Here I shall concentrate on the transport of energy. I do wish to point out that a whole previous conference has been devoted to this topic (Sawaya-Lacoste, 2002), so that the coverage given here will by necessity be brief and incomplete.

The magnetic field can transport and release energy in a variety of ways. One form of energy transport is through waves. The magnetic field supports a rich variety of wave modes. These are discussed in detail in a number of other presentations made at the SOHO 13 meeting (e.g. Roberts, 2003; Wang, 2003; Ofman, 2003; Nakariakov, 2003). Therefore, here I'll concentrate on other mechanisms (cf. Innes, 2003; Winebarger, 2003). These involve changes in the magnetic configuration which bring the field into a state in which curvature forces are significant, i.e. bring the field in to a state of higher energy. In many cases such changes are expected to lead to the formation of tangential discontinuities and null points (Parker, 1983, 1988; Longcope and Van Ballegooijen, 2002). At such locations this excess energy can be released through magnetic reconnection or through ohmic dissipation at a current sheet. In particular, magnetic reconnection changes the connectivity of the magnetic field lines. Since connectivity can be identified with topology, this implies a change in magnetic topology (see Sweet, 1958; Priest and Forbes, 2000).

I begin with a simple introduction to magnetic topology and reconnection, followed by a discussion of magnetic coupling and its drivers. Examples of the discussed processes are provided for illustration purposes.

2. MAGNETIC TOPOLOGY AND TOPOLOGICAL CHANGE

When dealing with localized parts of the solar atmosphere the magnetic field in the solar atmosphere can in simple terms be considered to fill a half space, with sources of magnetic energy distributed on the surface bounding this half-space. This boundary is generally taken to be the solar photosphere. Above the photosphere

Proc. of SOHO 13 'Waves, Oscillations and Small-Scale Transient Events in the Solar Atmosphere: A Joint View from SOHO and TRACE', Palma de Mallorca, Balearic Islands (Spain), 29 September – 3 October 2003 (ESA SP-547, January 2004)

the magnetic field is essentially force-free and above a certain level (thought to lie in the chromosphere) it fills all of the available space (Jones and Giovanelli, 1982; Anzer and Galloway, 1983; Solanki and Steiner, 1990). In contrast, at and below this layer a significant fraction of the magnetic field is bundled into discrete elements (often described in terms of magnetic flux tubes or flux sheets; i.e. Spruit et al., 1991; Solanki, 1993). Furthermore, the thermal pressure and dynamics of the gas also play an important role in determining the distribution of the magnetic field there.

In particular, in the lower photosphere the magnetic energy density is generally smaller than the thermal energy density of the field-free gas. This means that field lines cannot move at will through the photosphere and definitely not through the convection zone (unlike the situation in the corona). This leads to the idea of (nearly) immovable discrete sources of magnetic flux in the photosphere from which field lines emanate to fill the corona. This is obviously a simplification but a useful one and is often referred to as line tying.

The magnetic structure is relatively uninteresting as long as there are only 2 discrete sources. A 2-D sketch of the situation is shown in Figure 1a, following Bungey et al. (1996). In this case any field lines that start close together (i.e. from the one source), also end up close together (in the other source). With more discrete sources, more complex and interesting magnetic topologies are possible. In Figure 1b a situation is illustrated in which one field line just touches the solar surface between the two outer sources. The location where it lies parallel to the solar surface is called a bald patch. Field lines that lie above the solid line simply connect these two sources (indicated by upper dashed curve). Field lines that lie below it, however, return into the solar interior near the bald patch (lower dashed curve). Since the field lines lying on both sides of the solid line have very different connections, the solid line is a separatrix. In Figure 1c a situation with an X-point is sketched. The two solid lines are separatrices, as can easily be judged by considering the dashed lines which indicate field lines lying close to the solid lines. It is clear from Figure 1c that the X-point where the field disappears and the two separatrices intersect is the most likely location for magnetic reconnection to occur.

In 3-D the situation is more complex. This is evident when considering the structure of null points, i.e. 3-D counterparts of X-points, where the magnetic field disappears. One such structure is illustrated in Figure 2, which is adapted from Brown and Priest (2001). The two main features of the field around a null are the parallel field lines approaching the null from both sides. The central field line of these parallel bundles, passing through the null, is called the spine. The other main feature is the fan of expanding field lines leaving the null (nulls are also possible for which the directions of all the field lines are reversed). The central plane of the fan is a separatix surface. Note that field lines located point symmetrically to the null have opposite polarities and can reconnect across the null. A cut through a null along the spine (i.e. a vertical cut in Figure 2) reveals a picture very similar to that of an X-point in 2-D.

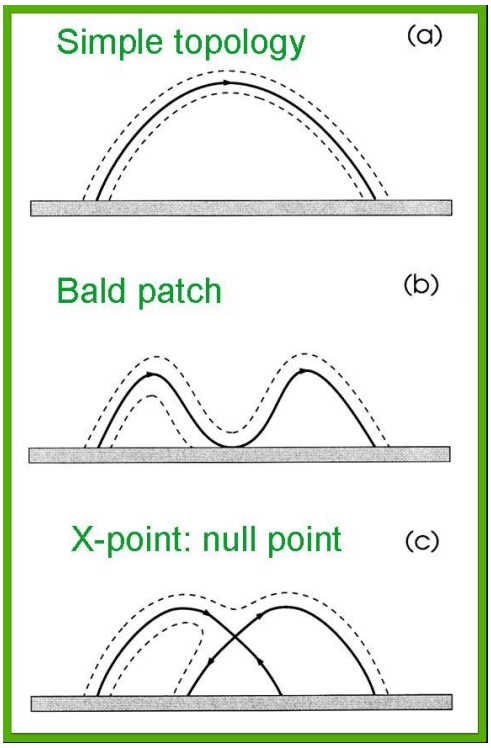

Figure 1. Schematic illustration of different magnetic topologies in 2-D. The shaded bar at the bottom of each figure represents the solar photosphere. Solid and dashed curves represent field lines. In (b) and (c) the solid curves correspond to separatrices (adapted from Bungey et al., 1996).

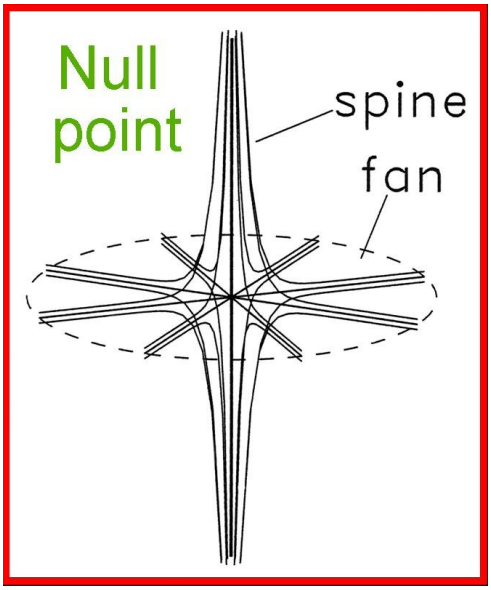

Figure 2. Illustration of the magnetic field lines around a 3-D null point (located at the intersection of the straight lines). The spine and fan structure are indicated (adapted from Brown and Priest, 2001).

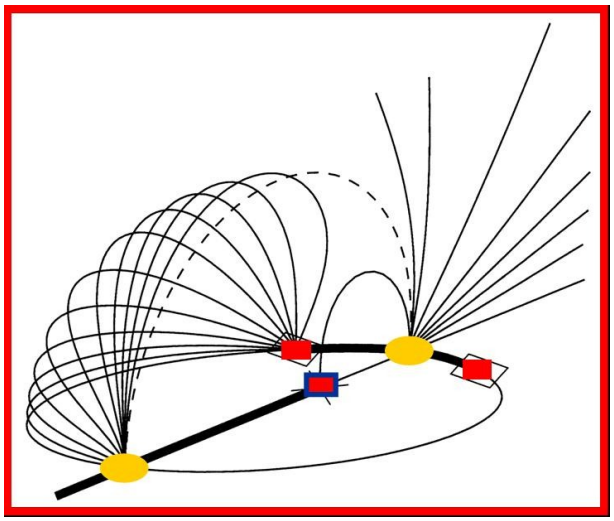

Figure 3. Magnetic skeleton for a simple case with 3 magnetic sources (red rectangles; the one with a dark blue border has opposite polarity to the other two). The 2 null points are marked by the yellow ovals, spine field lines by the thick black lines and field lines belonging to separatrices by thin solid curves (fans of null points). This particular skeleton harbours two different types of separatrices, a dome (on the left) and a wall (on the right). The separator is indicated by the dashed curve (adapted from Beveridge et al., 2002).

Taking the ingredients presented so far we can now describe what is often referred to as the magnetic skeleton of a region. The skeleton contains the features of the magnetic field that define its topology and are of relevance for magnetic reconnection and current dissipation. An illustration is given in Figure 3 for three magnetic sources (marked by boxes) and two null points (ovals; Beveridge et al. (2002)). The spines are marked by thick lines and the two separatrices are indicated by the solid field lines. Of particular interest is the dashed curve, called the separator. It is the intersection between two separatrices and is in this sense analogous to the X-point in 2-D (Figure 1). Separators are thought to be the location of current filament formation and possible magnetic reconnection. The topological structure of more complex or more specific magnetic configurations is of greater relevance for the real Sun. It has been investigated by many authors, e.g., Longcope and Van Ballegooijen (2002); Schrijver and Title (2002). The former authors have not only computed non-potential fields, but also have followed the evolution of the field, as it reacts to footpoint motions.

Evidence for reconnection along separators is provided by a number of studies (e.g., Longcope, 1996; Mandrini et al., 1996; Démoulin et al., 1997; Wang et al., 2000; Longcope et al., 2001). In Figure 4 we show an example taken from Démoulin et al. (1997). Note that although only 4 (extended) sources were employed (identified in the measured vector magnetogram of AR 2779) the extrapolation of the magnetic field is computed employing a force-free field. In Figure 4a the magnetogram is indicated by the contour lines, while O V flare kernels are represented by the shaded areas. In Figure 4b contours

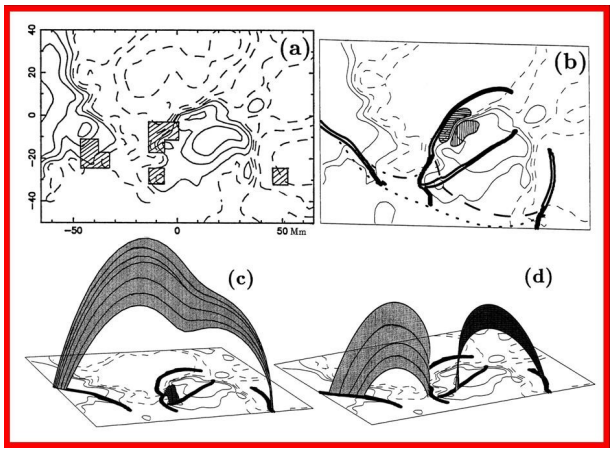

Figure 4. Magnetic skeleton obtained through force-free field extrapolations of AR 2779 and comparison with flare kernels. a) Contours of the longitudinal magnetic field with flare kernels seen in O V overplotted (shaded areas). b) Electric current density contours and intersections of the Quasi Separatrix Layers with the solar surface (thick lines). c) and d) Perspective views of Fig. b) with two Quasi Separatrix Layers (QSLs) plotted in each frame. The active region is found to have a total of 4 QSLs. (adapted from Démoulin et al., 1997).

of the current density are plotted. Also plotted are the intersections with the solar surface of QSLs (Quasi Separatrix Layers). A QSL is a layer across which the connectivity of field lines changes significantly, but without the presence of a null point. QSLs have been brought into connection with current dissipation and reconnection. In Figure 4c and d perspective views of the region are shown and the QSLs are plotted.

It is evident that both, the current density and the O V flaring kernels are located at or close to the intersection of the QSLs with the solar surface. Thus, the QSLs outline locations at which excess heating and/or flaring takes place. Techniques for determining the location of QSLs are becoming increasingly powerful and the QLS location, as deduced from force-free magnetic field extrapolations, agree well with locations in X-ray and EUV images at which loops part to follow different trajectories (e.g. Régnier et al., 2002a).

Although magnetic field extrapolations have in many cases proved to be a useful tool, it is important to test them and to validate them compared with actual observations. Generally such tests are carried out by comparing the computed field structure with either magnetic field strength maps obtained from radio observations or brightness maps (where brightness striations and loop-like strucures are thought to outline magnetic field lines, or rather their projection onto the image plane; e.g. Régnier et al. 2002b). The full magnetic vector was previously deduced from Hanle effect measurements, mainly in Prominances (e.g. Bommier, 1999) but also in a coronal hole (Raouafi et al., 2002). Unfortunately, such observations have so far been rare and are limited to these special structures.

Recently it became possible to directly measure the full magnetic vector in systems of cool loops with the help of

the He I 10830Å triplet. The structure of some magnetic loops deduced in this manner is plotted in Figure 5 (from Solanki et al. 2003, cf. Lagg et al. 2003). A comparison of these loops with potential and constant-α force-free calculations (Wiegelmann and Neukirch, 2002) reveals that the field is far from being potential, even in this very young active region and for this freshly emerged loop. This demonstrates that excess energy (i.e. in excess of that in the potential field configuration) is input into the coronal field not only through, e.g., field line braiding by footpoint motions (see Sects. 3 and 4), but may already be present in the magnetic structure directly at emergence of the field into the solar atmosphere.

3. CAUSES OF TOPOLOGICAL CHANGE

The causes of changes of the magnetic topology can be found either in the upper atmosphere itself or in the magnetic sources embedded in the photosphere. Consider first the upper atmosphere.

- Magnetic reconnection can be induced by reconnection at nearby sites. A prime example is given by the avalanche model of flares and the concept of self-organized criticality. (Lu and Hamilton, 1991; Lu, 1995a,b; Charbonneau et al., 2001). Another example is sympathetic flaring, i.e. flares occuring close in time in different active regions. Although in this case the connection between the different flaring sites has been argued to be subphotospheric (Fritzova-Svestkova et al., 1976; Moon et al., 2002).
- Another possible driver, or at least enhancer of reconnection is given by MHD waves. Evidence for this is found in time series of explosive events (Ning et al., 2003). At least in some cases these are found to repeat with a period of 3–5 minutes, which are typical for waves in the chromosphere and transition region. Waves can, by compressing the gas and the embedded field (or in the case of Alfvén waves by changing the angle between neighbouring field lines) periodically enhance the conditions for magnetic reconnection.

Note that these causes for topological changes located in the upper atmosphere are, at a more fundamental level, themselves driven by processes acting in the photosphere and solar interior. Perturbations in the lower atmosphere refer mainly to the strength (i.e. magnetic flux) and distribution of the photospheric sources of the coronal field. Such changes in the sources are produced by flows and motions in the photosphere and subphotosphere, which can be ordered according to the following headings:

- *Global flow fields*: these encompass solar rotation, meridional circulation and torsional oscillations.
- *Magnetic flux emergence*: driven by the buoyancy of flux tubes in the convection zone and influenced by the, e.g., magnetic curvature, aerodynamic drag and Coriolis forces acting on the rising flux tubes.
- *Large scale flows*: here meant to include giant cells, supergranulation and moat flows.
- *Small-scale flows*: granules and mesogranules, small-scale turbulent flows, flows within individual magnetic elements.

On short time scales (shorter than active region lifetimes) and for local changes of magnetic topology (i.e. length scales up to active region sizes) small-scale flows, supergrunules and the emergence of new flux are probably the main drivers. On scales larger than $2''$ the influences of these flows on photospheric magnetic elements are well visible in time series of MDI magnetograms. Since photospheric magnetic features often have diameters well below this scale (Solanki, 1993), it is important also to know the motions of the individual magnetic elements. This is not straightforward since the individual magnetic elements are generally spatially unresolved in magnetograms.

To obtain an idea of the dynamics at these very small scales one currently either considers proxies of the magnetic field (e.g. G-band time series, Berger et al., 1998a,b) or 3-D compressible radiation MHD simulations. Such simulations show intense magnetic elements concentrated into sheets that are being jostled by the granules and moving around as granules decay and new ones form (Vögler and Schüssler, 2003; Vögler et al., 2003). Such simulations have already been employed to show that the assumption that G-band bright points outline the magnetic flux concentrations is correct (Schüssler et al., 2003). Although individual magnetic features can be followed in great detail in numerical simulations, in general only a limited fraction of the motions present in the solar photosphere is present in any given simulation.

4. MAGNETIC COUPLING IN ACTION: PHOTOSPHERIC DRIVING, CURRENT SHEETS AND CORONAL HEATING

Recently Gudiksen and Nordlund (2002) have carried out a 3-D simulation of magnetic field evolution with a realistic boundary condition. Their work builds upon that of Galsgaard and Nordlund (1996) and of Galsgaard et al. (2000). Gudiksen and Nordlund (2002) considered an MDI magnetogram (Scherrer et al., 1995) which they then extrapolated into the corona assuming a potential field (see Figure 6, bottom panel). Using this as an initial condition they perturbed the magnetogram with a velocity spectrum similar to that expected from convection (v $\sim$ k, where k is the wavenumber). They included radiative losses in a simple way as well as thermal conductivity using Spitzer's formula.

Due to the perturbation of the photospheric field the magnetic field in the corona evolves, with the field lines getting braided, and current sheets are formed. Along these, DC current dissipation results in a heating of the involved loops. Gudiksen and Nordlund (2002) find maximum loop temperatures of up to 4MK and an average coronal temperature of 1-1.3 MK.

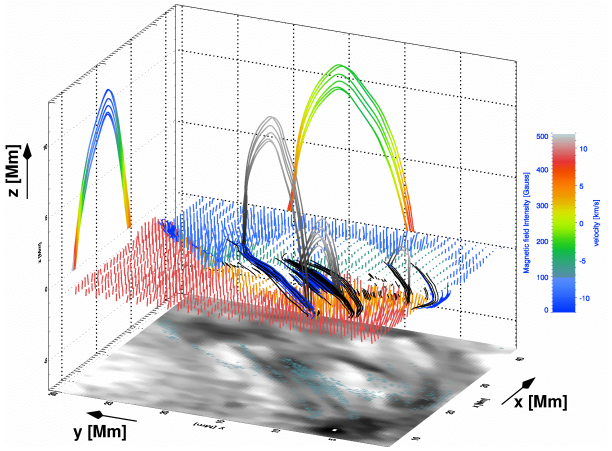

Figure 5. 3-D magnetic structure of selected loops (grey bundles of curves) in an emerging flux region. Magnetic polarities in the chromospheric magnetogram are represented by the colours in the plane at the footpoints of the loop (red-yellow: one polarity; blue-green: opposite polarity). Below that a brightness image in He I 10830 is plotted. The projection on the left shows the field strength, the projection on the right velocities in the largest reconstructed loop (from Solanki et al., 2003).

Gudiksen and Nordlund (2002) have also considered what the observed signature of these loops would be if seen by the TRACE 171Å channel (Handy et al., 1999). They find numerous narrow loops in their synthetic TRACE image, which agrees qualitatively with TRACE results. The actual magnetic loops are in general much broader (in agreement with the direct measurements of coronal fields, see Figure 5). The simulations show that the seeming narrowness of the TRACE loops is due to the narrow ΔT range sampled by the TRACE 171Å channel (Figure 6b).

The work of Parker (1972, 1982, 1983); Gudiksen and Nordlund (2002) and of others has highlighted the importance of current sheets or tangential discontinuities for coronal heating. Until recently no current sheet in the upper atmosphere had been found. Observations with He I 10830Å have, however, uncovered just such a structure (Solanki et al., 2003). In Figure 7 we plot the relevant data. The height of the peak denotes the field strength. Note the narrow, 1″ wide, valley marking the location of the current sheet. The width of this valley is mainly set by the seeing produced by turbulence in the Earth's atmosphere. This suggests that the current sheet is spatially not resolved. Also, the current densities indicated by the colouring of the figure are expected to be an underestimate.

Finally, I briefly consider the question of whether steady dissipation of currents is the dominant process by which the corona is heated, as first proposed by Parker (1972), or if it is rather nano-flare heating, i.e. heating by impulsive energy release.

The microflare hypothesis put forward initially by Parker (1982, 1983, 1988) has in general been tested by examining time series and identifying transient brightenings

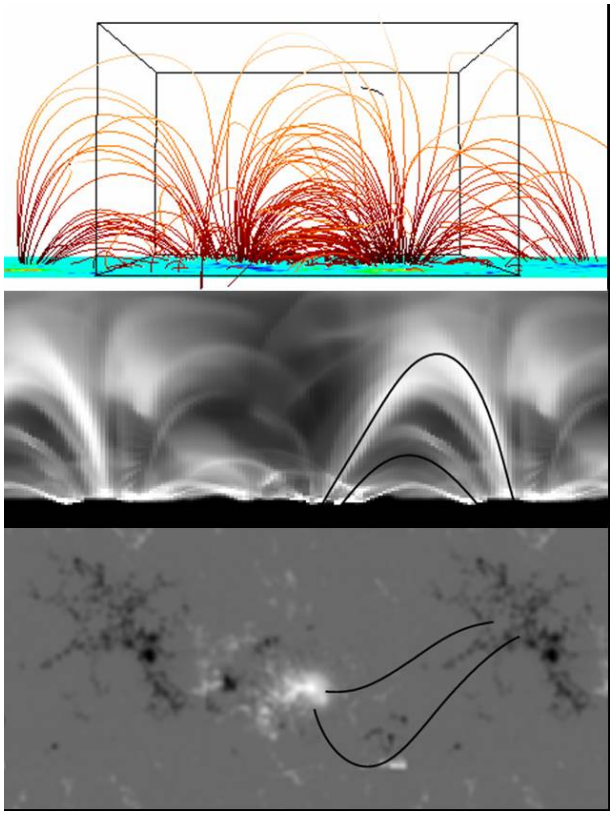

Figure 6. Computed magnetic field lines (top). Simulated off-limb TRACE 171Å channel image corresponding to a snapshot of the full simulation (middle), MDI magnetogram (bottom). Two field lines are marked in both the middle and lower figures. Note that one of them corresponds to a loop bright in TRACE 171Å the other one not (from Gudiksen and Nordlund, 2002).

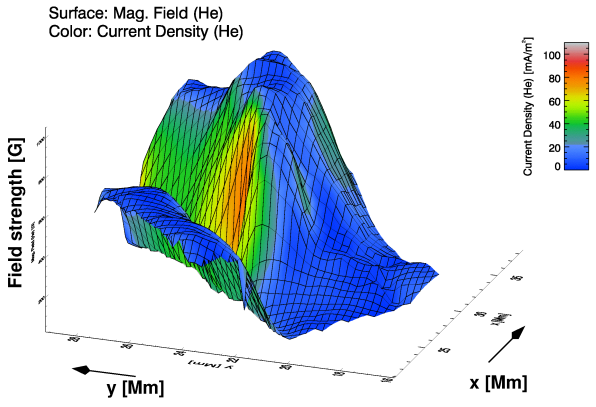

Figure 7. Electric current sheet located near the base of the corona between freshly emerged and previously present magnetic flux. The height of the plotted surface represents magnetic field strength. Note that fields on either side of the narrow valley have opposite polarities. The colours indicate the magnitude of the electric current flowing along the current sheet (adapted from Solanki et al., 2003).

corresponding to the larger nano-flares. From such analyses it is evident that nano- and microflare energies follow a power law distribution. Such investigations also seem to indicate that there isn't enough energy in the larger such events to heat the corona. The success of this model thus depends on the amount of energy in the small-scale events. This can be estimated from the power law exponent. If it is more positive than -2, then there isn't enough energy in nano-flares to heat the corona and compensate for radiative losses. In the case of smaller exponents sufficient energy may be present (Hudson, 1991). Numerous attempts have been made to determine the exponent from different types of data (e.g. Benz and Krucker, 2002; Krucker and Benz, 1998; Parnell and Jupp, 2000; Brković et al., 2001; Winebarger et al., 2002). The obtained values exhibit some scatter, with a tendency for the exponent to be more positive than -2 (see Winebarger 2003 for an overview). However, the very technique for estimating the exponent may tend to underestimate it, since a large number of weak events cause the brightenings to blend together, reducing the number of weak events (i.e. the micro and nanoflares) that can be individually identified and increasing the number of seemingly large events. Pauluhn and Solanki (2003) have taken an approach more similar to Hudson (1991). They assume a power law distribution of nano- and microflare energy and create an artificial time series from a random distribution in time. This is compared with observations obtained with the SUMER spectrometer (Wilhelm et al., 1995) and the free parameters entering the model are changed until a good agreement is reached. Preliminary results, presented by Pauluhn and Solanki (2003), suggest that values of the exponent more negative than -2 are compatible with the observations. However, a more in-depth analysis is required.

5. CONCLUSIONS

Magnetic coupling between different parts of the Sun plays a fundamental role in determining the structure, dynamics and thermodynamics of the upper solar atmosphere. Inspite of its crucial importance many aspects of magnetic coupling have as yet not been studied in detail. There is a particularly dire need for more and better observations of the magnetic field in the corona and near its base.

Of equal importance are co-temporal and co-spatial very high resolution observations in both the photosphere (mainly magnetic field measurements, but also images in selected wavelenght bands) and the transition region/corona. Observations of the photosphere of the type discribed above are exactly what the Sunrise balloon-borne observatory (Solanki et al., 2002) will provide. The Solar Orbiter mission of ESA will in some respects go a step further and will map both the photospheric magnetic field and the transition region and coronal rediation at an unprecedented spatial resolution of better than 100 km on the Sun (in the baseline plan for the mission). This should allow the relevant dynamics of photospheric magnetic features to be followed and the response of the upper solar atmosphere to these dynamics to be detected at the same time.

REFERENCES

Anzer U., Galloway D.J., *MNRAS* 203, 637, 1983.

Benz A.O. and Krucker S., *ApJ* 568, 413, 2002.

Berger T.E., Löfdahl M.G., Shine R.A., Title A.M., *ApJ* 495, 973, 1998a.

Berger T.E., Löfdahl M.G., Shine R.A., Title A.M., *ApJ* 505, 493, 1998b.

Beveridge C., Priest E.R., Brown D.S., *Sol. Phys.* 209, 333, 2002.

Bommier V., in *Ninth European Meeting on Solar Physics: Magnetic Fields and Solar Processes*, A. Wilson (Ed.), ESA SP-448, p. 95, 1999.

Brković A., Solanki S.K., Rüedi I., *A&A* 373, 1056, 2001.

Brown D.S. and Priest E.R., *A&A* 367, 339, 2001.

Bungey T.N., Titov V.S., Priest E.R., *A&A* 308, 233, 1996.

Charbonneau P., McIntosh S.W., Liu H.-L., Bogdan T.J., *Sol. Phys.* 203, 321, 2001.

Démoulin P., Bagala L.G., Mandrini C.H., Henoux J.E., Rovira M.G., *A&A* 325, 305, 1997.

Fritzova-Svestkova L., Chase R.C., Svestka Z., *Sol. Phys.* 48, 275, 1976.

Galsgaard K. and Nordlund Å, *JGR* 101, 13445, 1996.

Galsgaard K., Priest E.R., Nordlund Å., *Sol. Phys.* 193, 1, 2000.

Gudiksen B.V. and Nordlund Å., *ApJ* 572, L113, 2002.

Handy B.N. et al., *Sol. Phys.* 187, 229, 1999.

Hudson H.S., *Sol. Phys.* 133, 357, 1991.

Innes D., These proceedings, 2003.

Jones H., Giovanelli R.G. *Sol. Phys.* 87, 37, 1982.

Krucker S. and Benz A.O., *ApJ* 501, L213, 1998.

Lagg A., Woch J., Krupp N., Solanki S.K., *A&A* in press, 2003.

Longcope D.W., *Sol. Phys.* 169, 91, 1996.

Longcope D.W., Van Ballegooijen A.A., *ApJ* 578, 573, 2002.

Longcope D.W., Kankelborg C.C. Nelson J.L., Pevtsov A.A., *ApJ* 553, 429, 2001.

Lu E.T., *ApJ* 447, 416, 1995a.

Lu E.T., *ApJ* 446, L109, 1995b.

Lu E.T. and Hamilton R.J., *ApJ* 380, L89, 1991.

MacGregor K.B., Charbonneau P., in *Cool Stars, Stellar Systems and the Sun VIII*, J.-P. Caillault (Ed.), ASP Conf. Ser. Vol. 64, p. 174, 1994.

Mandrini C.H., Démoulin P., van Driel-Gestelyi L., Schmieder B., Cauzzi G., Hofmann A., *Sol. Phys.* 168, 115, 1996.

Mestel L., Spriut H.C., *MNRAS* 226, 57, 1987.

Moon Y.-J., Choe G.S., Park Y.D., et al., *ApJ* 574, 434, 2002.

Nakariakov V., These proceedings 2003.

Ning Z., Innes D., Solanki S.K., *A&A* submitted, 2003.

Ofman L., These proceedings, 2003.

Parnell C.E., Jupp P.E., *ApJ* 529, 554, 2000.

Parker E.N., *ApJ* 174, 499, 1972.

Parker E.N., *Geophys. Astrophys. Fluid Dyn.* 22, 195, 1982.

Parker E.N., *ApJ* 264, 642, 1983.

Parker E.N., *ApJ* 330, 474, 1988.

Pauluhn A. and Solanki S.K., These proceedings, 2003.

Priest E.R., and Forbes T., *Magnetic Reconnection: MHD Theory and Applications*, Cambridge Univ. Press, 2000.

Raouafi N.-E., Sahal-Bréchot S., Lemaire P., *A&A* 396, 1019, 2002.

Régnier S., Amari T., Canfield R.C., in *SOLMAG: Magnetic Coupling of the Solar Atmosphere*, IAU Colloq. 188, ESA SP-505, p. 65, 2002a.

Régnier S., Amari T., Kersalé E., *A&A* 392, 1119, 2002b.

Roberts B., These proceedings, 2003.

Sawaya-Lacoste H. (Ed.), *SOLMAG: Proc. Magnetic Coupling of the Solar Atmosphere*, Euroconference and IAU Colloquium 188, ESA SP-505, 2002.

Scherrer P.H., et al., *Sol. Phys.* 162, 129, 1995.

Schrijver C.J., Title A.M., *Sol. Phys.* 207, 223, 2002.

Schüssler M., Shelyag S., Berdyugina S., Vögler A., Solanki S.K., *ApJ* in press, 2003.

Solanki S.K., *Space Sci. Rev.* 63, 1, 1993.

Solanki S.K. Steiner O., *A&A* 234, 519, 1990.

Solanki S.K., Motamen S., Keppens R., *A&A* 324, 943, 1997.

Solanki S.K., et al. in *Proc. Magnetic Coupling of the Solar Atmosphere*, Euroconference and IAU Colloquium 188, Ed.: H. Sawaya-Lacoste, ESA SP-505, p. 27, 2002.

Solanki S.K., Lagg A., Woch J., Krupp N., Collados M., *Nature* 425, 692, 2003.

Spruit H.C., Schüssler M., Solanki S.K., in *Solar Interior and Atmosphere*, A.N. Cox et al. (Eds.), Univ. of Arizona Press, Tucson, p. 890, 1991.

Sweet P.A., in *Electromagnetical Phenomena in Cosmical Physics*, B. Lehnert (Ed.), Cambridge Univ. Press, p. 123, 1958.

Vögler A. and Schüssler M., *Astron. Nachr.* 324, 399, 2003.

Vögler A., Schüssler M., et al., A&A to be submitted, 2003.

Wang T.-J., These proceedings, 2003.

Wang H., Yan Y., Sakurai T., Zhang M., *Sol. Phys.* 197, 263, 2000.

Wiegelmann T., Neukrich T., *Sol. Phys.* 208, 233, 2002.

Wilhelm K. et al., *Sol. Phys.* 162, 189, 1995.

Winebarger A.R., Emslie A.G., Mariska J.T., Warren H.P., *ApJ* 565, 1298, 2002.

Winebarger A.R., These proceedings, 2003.